Overcoming the Diffraction Limit on the Size of Dielectric Resonators Using an Amplifying Medium

I. V. Doronin, E. S. Andrianov, and A. A. Zyablovsky [*]
Dukhov Research Institute of Automatics, 22 Sushchevskaya, Moscow 127055, Russia
and Moscow Institute of Physics and Technology, 9 Institutskiy pereulok, Moscow 141700, Russia

(Received 26 June 2022; accepted 12 September 2022; published 23 September 2022)

Existing methods for the creation of subwavelength resonators use either structures with negative permittivity, by exploiting subwavelength plasmonic resonances, or dielectric structures with a high refractive index, which reduce the wavelength. Here, we provide an alternative to these two methods based on a modification of the modes of dielectric resonators by means of an active medium. On the example of the dielectric active layer of size substantially smaller than a half-wavelength of light, we demonstrate that there is a gain at exceeding of which the change in phase due to the reflection at the layer boundaries compensates the change in phase due to propagation over the layer. Above this value of the gain, an unconventional mode forms, in which the phase shift after a round-trip of the light is zero. We show that this mode can be exploited to create a laser, the size of which is much smaller than the wavelength of the generated light and scales inversely with the square of absolute value of the refractive index in the active medium. Our results pave the way to creation of dielectric lasers of subwavelength size.

DOI: 10.1103/PhysRevLett.129.133901

Introduction.—Creation of subwavelength resonators and light localization are of great importance from the points of view of both the possible applications and fundamental physics. Among the practical applications are high-sensitivity sensors [1–4], biochemical microscopy and sensing [5–11], photonics, and optoelectronics [12–20]. The common theme in these applications is focusing light within a small volume, either for high-precision measurements or fast response times. There is also interest in the theoretical investigation and experimental creation of strong [21–33] and ultrastrong light-matter interactions [34–36].

The use of dielectric structures for subwavelength localization has been deemed impossible, since the Helmholtz equation restricts the minimal possible size of a cavity based on a dielectric structure placed in a vacuum. For example, the cavity based on a dielectric slab without gain and loss needs to be at least as large as $l_0 = \lambda/2\sqrt{\varepsilon}$ [37], where ε is the layer permittivity. In this case, the phase acquired by the light after a full round-trip over the cavity is equal to 2π. Similar restrictions apply to other types of dielectric resonator—for example, dielectric Mie particles [38]. Using materials with high values of permittivity enables the cavity size to be reduced [38–43]. Despite practical significance [38–40,44–48], this approach provides a quantitative rather than a qualitative solution to the problems arising due to the diffraction limit. In optics, the additional limitation of this method is that the refractive indexes of known materials are limited to small numbers ($n \sim 4$) [38].

The subwavelength localization of electromagnetic fields can be achieved via surface plasmon resonances [1,2,8–12,19,20,49–54]. This type of resonance only arises in structures containing materials with both positive and negative permittivity. This enables eigenmodes in which the amplitude of the electric field reaches a maximum near the interface between two materials with permittivities of opposite signs and decreases with the distance from this interface [53]. At appropriate values of the permittivity, this decay causes subwavelength localization of light. However, plasmonic nanostructures typically have large ohmic losses [55,56], which gives rise to the necessity of using gain materials for nanoscale light localization.

Until recently the gain media used in such structures have been considered as materials that only reduce the losses in the electromagnetic (EM) modes formed by the dielectric or plasmonic structure itself [56–58]. It has only recently been understood that gain materials can substantially change the eigenmodes of the optical system [59,60]. For example, the use of amplifying and absorbing layers allows for the creation of an optical parity-time symmetrical structure [61–75], in which the change in the gain coefficient can lead to a spontaneous symmetry breaking of the eigenstates [62,63,65]. The use of these structures makes it possible to create new types of lasers [26,33,60,76–80], sensors [81–84], and waveguide systems [85–88].

Inspired by these achievements, the question arises as to whether it is possible to create a dielectric resonator of subwavelength size by using an active medium. In this Letter, we give a positive answer to this question. We show for the first time that an active medium promotes the formation of a gain-assisted (GA) mode that is characterized by a zero phase shift of the EM wave after

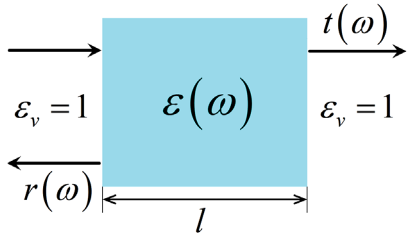

FIG. 1. Scheme of the system under consideration: a single layer with gain placed in free space. The relative permittivity in the gain layer is $\varepsilon(\omega) = \varepsilon'(\omega) + i\varepsilon''(\omega)$ where $\varepsilon''(\omega) < 0$. The relative permittivity of free space $\varepsilon_v = 1$.

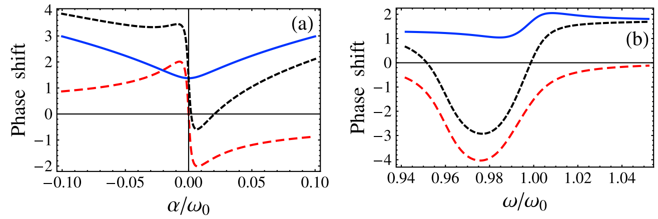

FIG. 2. Dependence of the phase shifts $\Delta\phi_{\rm pr}$ (solid blue line), $\Delta\phi_{\rm ref}$ (dashed red line), $\Delta\phi_{\rm tot} = \Delta\phi_{\rm pr} + \Delta\phi_{\rm ref}$ (dotted black line) on (a) α at the transition frequency, $\omega = \omega_0$; (b) on the frequency ω in the case of an amplifying medium, $\alpha = 0.02\omega_0$. The parameters are $\gamma = 0.01\omega_0$; $\varepsilon_0 = 1.2$; $l = 0.1\lambda_0$, where $\lambda_0 = 2\pi c/\omega_0$.

a full round-trip over the cavity. This mode can exist in an active dielectric layer of thickness much smaller than one half-wavelength of light in the medium. We propose a concept of a dielectric laser of subwavelength size based on the GA mode.

Scattering matrix for a dielectric layer with active medium.—We study the scattering of EM waves by a dielectric layer of thickness l placed in free space (Fig. 1). We consider that the layer is made of an isotropic material described by a complex relative permittivity $\varepsilon(\omega)$ and a relative permeability $\mu = 1$. Because of the isotropy of the material, the scattering is the same for both light polarizations and we consider only one of them.

The scattering matrix for this system is [89]

$$S(\omega) = \begin{bmatrix} r_L(\omega) & t(\omega) \\ t(\omega) & r_R(\omega) \end{bmatrix}, \quad (1)$$

where $t(\omega)$ is the transmission coefficient, and $r_L(\omega)$ and $r_R(\omega)$ are the reflection coefficients from the left and right sides of the layer, respectively. Because of the mirror symmetry of the system, these coefficients are equal to each other, $r_L(\omega) = r_R(\omega) = r(\omega)$. The transmission coefficients in the two opposite directions are equal to each other as well, in accordance with the Lorentz reciprocity theorem [90].

The transmission and reflection coefficients, and, accordingly, the scattering matrix of active layer have poles at certain frequencies ω_k determined by the following well-known condition [91,92]:

$$\left(\frac{\sqrt{\varepsilon_k' + i\varepsilon_k''} - 1}{\sqrt{\varepsilon_k' + i\varepsilon_k''} + 1}\right)^2 \exp\left(2i\frac{\omega_k}{c}\sqrt{\varepsilon_k' + i\varepsilon_k''}l\right) = 1. \quad (2)$$

Here, $\varepsilon(\omega_k) = \varepsilon_k' + i\varepsilon_k''$ is the layer permittivity and ε_k' and ε_k'' are the real and imaginary parts of the permittivity at the pole frequency ω_k.

For an absorbing layer, the frequencies of all poles are in the lower half of the complex frequency plane. An increase in the gain in the active medium causes the poles to move upward in the complex frequency plane. When at least one of the poles lies in the upper half of the complex frequency plane, lasing takes place in the system [76,89,91,92].

The Eq. (2) condition is reduced to amplitude and phase conditions [91,93,94]. The amplitude condition is obtained by taking the modulus of both sides of Eq. (2) [91] and corresponds to compensation radiation loss by amplification [91,93,94]. The phase condition requires that the phase shift of the EM field per one round-trip over the layer is a multiple of 2π [91,93,94], i.e.,

$$\frac{\omega_k}{c}\mathrm{Re}\sqrt{\varepsilon_k' + i\varepsilon_k''}l + \arg\left(\frac{\sqrt{\varepsilon_k' + i\varepsilon_k''} - 1}{\sqrt{\varepsilon_k' + i\varepsilon_k''} + 1}\right) = \pi m, \quad (3)$$

where m is an integer.

The existence of a Fabry-Perot mode in the layer is associated with fulfillment of the Eq. (3) phase condition, which determines the frequencies of the modes. It is usually assumed that the minimal thickness of a layer that supports a Fabry-Perot mode is $l_0 = \lambda/(2\mathrm{Re}\sqrt{\varepsilon})$. Therefore, the minimal size of the dielectric resonator appears to be limited by the diffraction. However, the resonant Eq. (3) phase condition is formally satisfied for $m = 0$. In this case, the phase shift of the EM field for each round-trip over the layer is zero. For a passive layer, this situation corresponds to zero layer thickness $l = 0$ and therefore the resonance for $m = 0$ is usually disregarded.

Below we show for the first time that in the presence of the negative imaginary part of permittivity, resonance for $m = 0$ becomes possible for a layer of finite thickness.

Condition for the existence of a gain-assisted mode in the subwavelength layer.—The Eq. (3) phase condition for $m = 0$ means that the total phase acquired after one round-trip inside the cavity is equal to zero. This total phase shift $\Delta\phi$ is equal to the sum of the phase shifts arising from propagation $\Delta\phi_{\rm pr} = 2l\mathrm{Re}[\sqrt{\varepsilon(\omega)}]\omega/c = 4\pi l\mathrm{Re}[\sqrt{\varepsilon(\omega)}]/\lambda$ and from reflection, $\Delta\phi_{\rm ref}(\omega) = 2\arg(\sqrt{\varepsilon(\omega)} - 1/\sqrt{\varepsilon(\omega)} + 1)$.

In a finite layer ($l > 0$) without both amplifying and absorbing medium ($\mathrm{Im}\varepsilon = 0$), the zero phase shift condition is not satisfied. Indeed, for a dielectric layer with $\varepsilon > 1$ placed in a vacuum with $\varepsilon_v = 1$, we have $\Delta\phi_{\rm pr} = 2l\sqrt{\varepsilon(\omega)}\omega/c = 4\pi l\sqrt{\varepsilon(\omega)}/\lambda > 0$, whereas $\Delta\phi_{\rm ref} = 0$.

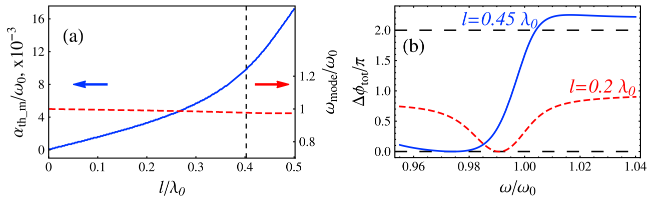

FIG. 3. (a) Dependence of the threshold of GA mode formation ($\alpha_{\text{th\_m}}$) in a dielectric layer of thickness l. The solid blue line shows the threshold value of $\alpha_{\text{th\_m}}$, and the dashed red line is the mode frequency at $\alpha = \alpha_{\text{th\_m}}$. The vertical dashed black line shows the layer thickness above which the Fabry-Perot mode with $m = 1$ exists in the passive layer ($\alpha = 0.0$). (b) Dependence of the total phase shift arising after one round-trip inside a layer of thickness l on the frequency. The solid blue line shows the dependence for $l = 0.45\lambda_0$; $\alpha = 0.013\omega_0$. The dashed red line shows the dependence for $l = 0.2\lambda_0$; $\alpha = 0.00326\omega_0$. $\gamma = 0.01\omega_0$ and $\varepsilon_0 = 1.2$. The horizontal dashed lines show the phase conditions for the GA mode ($\Delta\phi_{\text{tot}} = 0$) and the Fabry-Perot mode ($\Delta\phi_{\text{tot}} = 2\pi$).

Hence, to satisfy the resonance condition, $\Delta\phi_{\text{pr}}$ must be at least as large as 2π. In other words, the size of the dielectric layer needs to be at least half of the wavelength of light in the medium.

This situation changes significantly if the permittivity has a negative imaginary part. To be specific, we consider the active medium of two-level atoms, which is described by the following permittivity with Lorentzian dispersion [91,95]:

$$\varepsilon(\omega) = \varepsilon_0 + \frac{\alpha}{\omega - \omega_0 + i\gamma}. \tag{4}$$

The Eq. (4) permittivity can be derived from the Maxwell-Bloch equations [91] for the electromagnetic field and the medium of two-level atoms (see Supplemental Material [96]), and obeys the Kramers-Kronig relations [91,97]. Here, ε_0 is the permittivity of the medium where two-level atoms are embedded ($\varepsilon_0 > 0$); ω_0 and γ are the transition frequency and the linewidth of the two-level atoms, respectively. $\alpha > 0$ ($\text{Im}\varepsilon(\omega_0) < 0$) in the case of an amplifying medium and $\alpha < 0$ in the case of an absorbing medium.

Using the Eq. (4) expression, we calculate the dependencies of the phase shifts arising from reflection, $\Delta\phi_{\text{ref}}$, and the propagation, $\Delta\phi_{\text{pr}}$, on α [Fig. 2(a)]. It can be seen that the phase shift $\Delta\phi_{\text{ref}}$ [red dashed line in Fig. 2(a)] is negative for $\alpha > 0$, i.e., for an amplifying medium. The phase shift arising during propagation, $\Delta\phi_{\text{pr}}$, remains positive for all α [blue solid line in Fig. 2(a)] because it depends only on the real part of the wave vector, $k(\omega) = \omega\sqrt{\varepsilon(\omega)}/c$. As a result, using an active medium with a suitable value of α makes it possible to compensate for the phase shift arising from propagation by the phase shift on reflection. In this case, the total phase shift [black dotted line in Fig. 2(a)] arising after one round-trip inside the cavity can be equal to zero. This enables resonance in a subwavelength dielectric layer of nonzero thickness. We call this resonance a gain-assisted (GA) mode. Note that Fabry-Perot resonance with the zero phase shift also can be obtained in the dielectric layer adjacent to a metal surface ($\varepsilon' < 0$) [98]. The reflection from metal-dielectric boundary shifts phase by $-\pi$. This can be used to compensate the phase shift arising from propagation over the dielectric layer. However, to compensate for the phase shift the thickness of the dielectric layer alone should be about $\lambda/4\sqrt{\varepsilon'}$.

We can calculate the value of α at which $\Delta\phi_{\text{tot}} = \Delta\phi_{\text{pr}} + \Delta\phi_{\text{ref}}$ is zero for the given thicknesses of the active layer, i.e., we can find the threshold for the GA mode formation, $\alpha_{\text{th\_m}}$. As can be seen from Fig. 3(a) (solid blue line), this mode can form even when the layer thickness is much smaller than one half-wavelength. The frequency dispersion in the permittivity of the active medium [see Eq. (4)] ensures that at $\alpha > \alpha_{\text{th\_m}}$ the Eq. (3) phase condition is always fulfilled at some frequency near the transition frequency [see dotted black lines in Fig. 2(b)].

Notably, when the layer thickness exceeds one half-wavelength in the dielectric, the first Fabry-Perot mode

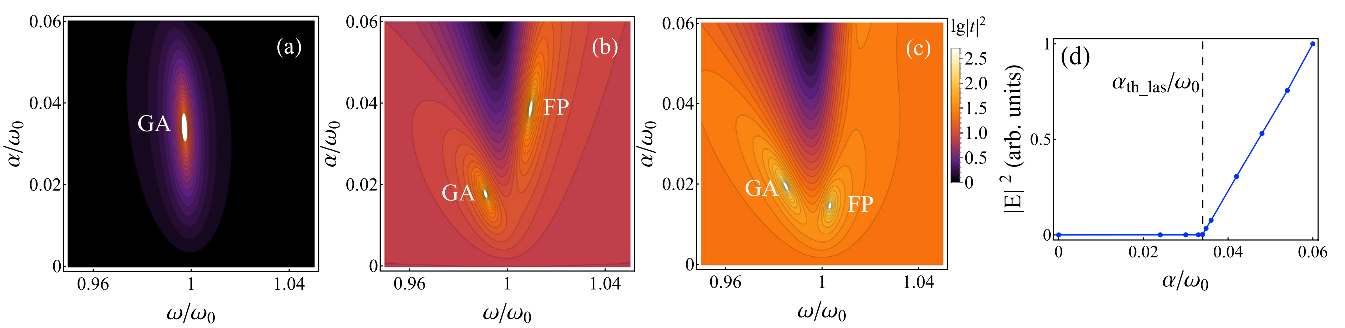

FIG. 4. (a)–(c) Dependencies of the decimal logarithm of the transmission $|t|^2$ [91] on ω and α. The layer thicknesses are (a) $l = 0.1\lambda_0$; (b) $l = 0.3\lambda_0$; and (c) $l = 0.45\lambda_0$. The letters GA and FP are used to mark the poles of the transmission coefficient corresponding to the gain-assisted mode and the Fabry-Perot mode, respectively. (d) Dependence of the intensity of electromagnetic field at the center of the layer of thickness $l = 0.1\lambda_0$ in the absence of an incident wave on α. The vertical dashed line shows the lasing threshold determined by the poles of the transmission coefficient [Fig. 4(a)]. $\varepsilon_0 = 1.2$.

($\Delta\phi_{\text{tot}} = 2\pi$) appears in the layer [solid blue line in Fig. 3(b)]. This mode exists for both negative and positive α. That is, in contrast to the GA mode, the gain is not necessary for the existence of the Fabry-Perot mode. For $\alpha > \alpha_{\text{th\_m}}$ and when the layer thickness exceeds one half-wavelength in the dielectric, both the GA mode and the conventional Fabry-Perot mode exist in the layer. The frequency of the GA mode [dashed red line in Fig. 3(a)] barely depends on the layer thickness, and is primarily determined by the transition frequency of the amplifying medium, while the frequencies of the conventional Fabry-Perot modes strongly depend on the layer thickness.

Lasing in the GA mode.—Above, we showed that the use of the active medium enables the GA mode in the subwavelength dielectric layer as long as the Eq. (3) phase condition is fulfilled for $m = 0$. However, the fulfillment of the Eq. (3) phase condition is not sufficient for lasing, which occurs when the frequency of at least one of the poles of the scattering matrix lies in the upper half of the complex frequency plane [76,89,91,92].

Using Eq. (2), we find the poles of the scattering matrix (Fig. 4) and the lasing threshold for different layer thicknesses [Fig. 5(a)]. The lasing threshold $\alpha_{\text{th\_las}}$ is determined as the minimal value of the imaginary part of the permittivity at which the frequency of one of the scattering matrix poles becomes real [76,89,91]. Our calculations show that depending on the layer thickness, lasing occurs either in the GA mode or in the conventional Fabry-Perot modes (Fig. 4). The GA mode threshold precedes the Fabry-Perot mode threshold when the layer thickness is less than one half-wavelength in the dielectric [Figs. 4(a) and 4(b)]. In this case, lasing occurs in the GA mode.

Lasing in the GA mode is possible even when the thickness of the dielectric layer with the active medium is much smaller than one half-wavelength of light in the medium [Fig. 5(a)]. The lasing threshold in this case is inversely proportional to the layer thickness [gray line in Fig. 5(a)]. Above the lasing threshold, the light generation occurs. The numerical simulation of the Maxwell-Bloch equations (see Supplemental Material [96]) shows that the laser at GA mode demonstrates the conventional lasing curve despite the thickness of the dielectric layer used as a cavity being much smaller than one half-wavelength [Fig. 4(d)]. The threshold obtained in the Maxwell-Bloch equations coincides with the threshold found from Eq. (2).

The GA mode has different dependence of the layer thickness at which lasing starts on the absolute value of the refractive index compared with the Fabry-Perot modes. In the case of the conventional Fabry-Perot modes, the phase condition at the transition frequency ω_0 is fulfilled when $l = m\lambda_0/[2n(\omega_0)]$, where $\lambda_0 = 2\pi c/\omega_0$ is the wavelength in free space at the transition frequency ω_0, $|n(\omega_0)| = |\sqrt{\varepsilon(\omega_0)}|$ is the absolute value of the refractive index, and m is an integer. It is generally considered that the gain shifts the resonance frequency only slightly. In this case, to create

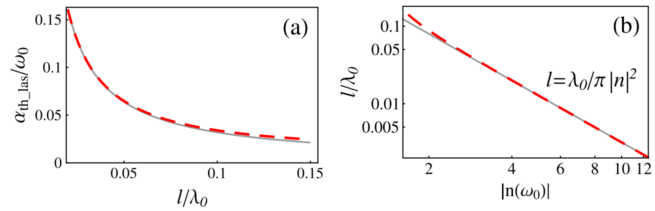

FIG. 5. (a) Dependence of the lasing threshold $\alpha_{\text{th\_las}}$ of GA mode on the layer thickness l (dashed red line). The gray line shows fitting of the lasing threshold dependence by l^{-1}. (b) Dependence of the layer thickness l on the absolute value of the refractive index $|n(\omega_0)| = |\sqrt{\varepsilon(\omega_0)}|$ at which lasing at GA mode starts (dashed red line). The solid gray line is $l = \lambda_0/\pi|n|^2$. Here, $\varepsilon_0 = 1.2$; $\gamma = 0.01\omega_0$.

a dielectric laser of thickness $l < \lambda_0/2$, it is necessary to use a material with $|n(\omega_0)| \approx \lambda_0/(2l)$. That is, the thickness of the dielectric laser scales as $1/|n(\omega_0)|$. For the GA mode, the dependence of the layer thickness on the absolute value of the refractive index is sharper [dashed red line in Fig. 5(b)] and at $|n(\omega_0)| \gg 1$ it can be approximated by $l = \lambda_0/\pi|n(\omega_0)|^2$ [solid gray line in Fig. 5(b)]. Hence, lasing in the GA mode can take place in a dielectric layer of thickness $l \ll \lambda_0/2|n(\omega_0)|$.

We can therefore conclude that an active dielectric layer of thickness much smaller than one half-wavelength of light in the medium can serve as a laser resonator.

To determine the experimentally achievable dielectric laser size, we calculate the gain corresponding to the lasing threshold [Fig. 5(a)]. For this purpose, we use the expression relating gain and permittivity $G = -2\omega \text{Im}\sqrt{\varepsilon(\omega)}/c$ [99]. Currently, experimentally achievable gain is of the order 10^5 cm^{-1} [93,100–102]. At a wavelength of 1500 nm, $\varepsilon_0 = 1.2$ and $\gamma = 0.1\omega_0$, the gain of 10^5 cm^{-1} corresponds to $\alpha \approx 0.39\omega_0$. At these parameters, the lasing can be achieved in the layer with thickness of $0.09\lambda_0$. This layer thickness is much smaller than one half-wavelength of light in the medium, which indicates the possibility of overcoming the diffraction limit using currently existing amplifying media.

Conclusion.—We have established a new type of modes in dielectric structures with an amplifying medium that makes it possible to overcome the diffraction limit on the size of dielectric structures. We consider a dielectric active layer with a thickness substantially smaller than the half-wavelength of light in the dielectric medium, and demonstrate that the use of an amplifying medium enables the formation of a gain-assisted (GA) mode characterized by a zero round-trip phase shift for the EM wave. This is achieved because the phase change on reflection at the boundaries of the active medium and the vacuum compensates the change in phase due to propagation over the layer. Therefore, the amplifying medium plays the key role in the GA mode formation. Our calculations (see Supplemental Material [96]) show that in the GA mode the energy is transferred from the electric field energy to the energy of active atoms and comes back. This behavior is similar to the formation of the plasmonic resonances in the subwavelength dielectric-metal structures that is due to the energy being transferred from the electric field energy to the energy of the electronic oscillations in the metal and coming back [55].

We demonstrate that there is a gain above which GA mode lasing in the subwavelength dielectric layer takes place. The lasing frequency is about equal to the transition frequency in the active medium ω_0. The thickness of the layer l supporting GA mode lasing is about $\lambda_0/\pi|n(\omega_0)|^2$. This behavior differentiates the laser based on GA mode from known types of dielectric lasers [103–107], where the thickness is about $\lambda_0/2|n(\omega_0)|$.

Thus, the use of the amplifying media enables us to achieve lasing based on resonator with subwavelength size. This opens the way for a new generation of subwavelength-sized dielectric lasers and sensors. Avoiding metal structures in proposed nanosized lasers can promote their integration with semiconductor electronic devices on the chip.

This study was financially supported by a grant from the Russian Science Foundation (Project No. 20-72-10057).

*Corresponding author.
zyablovskiy@mail.ru

[1] M. E. Stewart, C. R. Anderton, L. B. Thompson, J. Maria, S. K. Gray, J. A. Rogers, and R. G. Nuzzo, Nanostructured plasmonic sensors, Chem. Rev. **108**, 494 (2008).

[2] J. Homola, S. S. Yee, and G. Gauglitz, Surface plasmon resonance sensors: Review, Sens. Actuators B **54**, 3 (1999).

[3] J. Langer *et al.*, Present and future of surface-enhanced raman scattering, ACS Nano **14**, 28 (2020).

[4] P. Melentiev, A. Kalmykov, A. Gritchenko, A. Afanasiev, V. Balykin, A. S. Baburin, E. Ryzhova, I. Filippov, I. A. Rodionov, I. A. Nechepurenko, A. V. Dorofeenko, I. Ryzhikov, V. A. P., A. A. Zyablovsky, E. S. Andrianov, and A. A. Lisyansky, Plasmonic nanolaser for intracavity spectroscopy and sensorics, Appl. Phys. Lett. **111**, 213104 (2017).

[5] S. W. Hell and J. Wichmann, Breaking the diffraction resolution limit by stimulated emission: Stimulated-emission-depletion fluorescence microscopy, Opt. Lett. **19**, 780 (1994).

[6] S. W. Hell, Far-field optical nanoscopy, Science **316**, 1153 (2007).

[7] M. Fernandez-Suarez and A. Y. Ting, Fluorescent probes for superresolution imaging in living cells, Nat. Rev. Mol. Cell Biol. **9**, 929 (2008).

[8] K. Aslan, J. R. Lakowicz, and C. D. Geddes, Plasmon light scattering in biology and medicine: New sensing approaches, visions and perspectives, Curr. Opin. Chem. Biol. **9**, 538 (2005).

[9] J. Homola, Present and future of surface plasmon resonance biosensors, Anal. Bioanal. Chem. **377**, 528 (2003).

[10] K. A. Willets and R. P. van Duyne, Localized surface plasmon resonance spectroscopy and sensing, Annu. Rev. Phys. Chem. **58**, 267 (2007).

[11] A. G. Brolo, Plasmonics for future biosensors, Nat. Photonics **6**, 709 (2012).

[12] S. A. Maier, M. L. Brongersma, P. G. Kik, S. Meltzer, A. A. G. Requicha, and H. A. Atwater, Plasmonics—a route to nanoscale optical devices, Adv. Mater. **13**, 1501 (2001).

[13] R. F. Oulton, V. J. Sorger, D. A. Genov, D. F. P. Pile, and X. Zhang, A hybrid plasmonic waveguide for subwavelength confinement and long-range propagation, Nat. Photonics **2**, 496 (2008).

[14] A. L. Pyayt, B. Wiley, Y. Xia, A. Chen, and L. Dalton, Integration of photonic and silver nanowire plasmonic waveguides, Nat. Nanotechnol. **3**, 660 (2008).

[15] A. V. Krasavin and A. V. Zayats, Silicon-based plasmonic waveguides, Opt. Express **18**, 11791 (2010).

[16] X. Guo, Y. Ma, Y. Wang, and L. Tong, Nanowire plasmonic waveguides, circuits and devices, Laser Photonics Rev. **7**, 855 (2013).

[17] M. T. Hill, M. Marell, E. S. Leong, B. Smalbrugge, Y. Zhu, M. Sun, P. J. van Veldhoven, E. J. Geluk, F. Karouta, Y.-S. Oei, R. Notzel, C.-Z. Ning, and M. K. Smit, Lasing in metal-insulator-metal sub-wavelength plasmonic waveguides, Opt. Express **17**, 11107 (2009).

[18] E. Bermudez-Urena, G. Tutuncuoglu, J. Cuerda, C. L. Smith, J. Bravo-Abad, S. I. Bozhevolnyi, F. i. M. A., G.-V. F. J., and R. Quidant, Plasmonic waveguide-integrated nanowire laser, Nano Lett. **17**, 747 (2017).

[19] E. Ozbay, Plasmonics: Merging photonics and electronics at nanoscale dimensions, Science **311**, 189 (2006).

[20] M. Kauranen and A. V. Zayats, Nonlinear plasmonics, Nat. Photonics **6**, 737 (2012).

[21] D. G. Baranov, M. Wersall, J. Cuadra, T. J. Antosiewicz, and T. Shegai, Novel nanostructures and materials for strong light-matter interactions, ACS Photonics **5**, 24 (2018).

[22] G. Zengin, M. Wersall, S. Nilsson, T. J. Antosiewicz, M. Kall, and T. Shegai, Realizing Strong Light-Matter Interactions Between Single-Nanoparticle Plasmons and Molecular Excitons at Ambient Conditions, Phys. Rev. Lett. **114**, 157401 (2015).

[23] R. Chikkaraddy, B. de Nijs, F. Benz, S. J. Barrow, O. A. Scherman, E. Rosta, A. Demetriadou, P. Fox, O. Hess, and J. J. Baumberg, Single-molecule strong coupling at room temperature in plasmonic nanocavities, Nature (London) **535**, 127 (2016).

[24] B. Munkhbat, M. Wersall, D. G. Baranov, T. J. Antosiewicz, and T. Shegai, Suppression of photo-oxidation of organic chromophores by strong coupling to plasmonic nanoantennas, Sci. Adv. **4**, eaas9552 (2018).

[25] I. V. Doronin, A. S. Kalmykov, A. A. Zyablovsky, E. S. Andrianov, B. N. Khlebtsov, P. N. Melentiev, and V. I. Balykin, Resonant concentration-driven control of dye molecule photodegradation via strong optical coupling to plasmonic nanoparticles, Nano Lett. **22**, 105 (2022).

[26] I. V. Doronin, A. A. Zyablovsky, E. S. Andrianov, A. A. Pukhov, and A. P. Vinogradov, Lasing without inversion due to parametric instability of the laser near the exceptional point, Phys. Rev. A **100**, 021801(R) (2019).

[27] I. V. Vovchenko, V. Y. Shishkov, A. A. Zyablovsky, and E. S. Andrianov, Model for the description of the relaxation of quantum-mechanical systems with closely spaced energy levels, JETP Lett. **114**, 51 (2021).

[28] P. Torma and W. L. Barnes, Strong coupling between surface plasmon polaritons and emitters: A review, Rep. Prog. Phys. **78**, 013901 (2015).

[29] T. Yoshie, A. Scherer, J. Hendrickson, G. Khitrova, H. M. Gibbs, G. Rupper, C. Ell, O. B. Shchekin, and D. G. Deppe, Vacuum Rabi splitting with a single quantum dot in a photonic crystal nanocavity, Nature (London) **432**, 200 (2004).

[30] J. P. Reithmaier, G. Sek, A. Loffler, C. Hofmann, S. Kuhn, S. Reitzenstein, L. V. Keldysh, V. D. Kulakovskii, T. L. Reinecke, and A. Forchel, Strong coupling in a single quantum dot-semiconductor microcavity system, Nature (London) **432**, 197 (2004).

[31] K. Hennessy, A. Badolato, M. Winger, D. Gerace, M. Atature, S. Gulde, S. Falt, E. L. Hu, and A. Imamoglu, Quantum nature of a strongly coupled single quantum dot-cavity system, Nature (London) **445**, 896 (2007).

[32] F. Benz, M. K. Schmidt, A. Dreismann, R. Chikkaraddy, Y. Zhang, A. Demetriadou, C. Carnegie, H. Ohadi, B. De Nijs, R. Esteban, J. Aizpurua, and J. J. Baumberg, Single-molecule optomechanics in picocavities, Science **354**, 726 (2016).

[33] I. V. Doronin, A. A. Zyablovsky, and E. S. Andrianov, Strong-coupling-assisted formation of coherent radiation below the lasing threshold, Opt. Express **29**, 5624 (2021).

[34] T. Niemczyk, F. Deppe, H. Huebl, E. P. Menzel, F. Hocke, M. J. Schwarz, J. J. Garcia-Ripoll, D. Zueco, T. Hummer, E. Solano, A. Marx, and R. Gross, Circuit quantum electrodynamics in the ultrastrong-coupling regime, Nat. Phys. **6**, 772 (2010).

[35] A. F. Kockum, A. Miranowicz, S. De Liberato, S. Savasta, and F. Nori, Ultrastrong coupling between light and matter, Nat. Rev. Phys. **1**, 19 (2019).

[36] P. Forn-Diaz, L. Lamata, E. Rico, J. Kono, and E. Solano, Ultrastrong coupling regimes of light-matter interaction, Rev. Mod. Phys. **91**, 025005 (2019).

[37] M. Born and E. Wolf, *Principles of Optics: Electromagnetic Theory of Propagation, Interference and Diffraction of Light* (Elsevier, New York, 2013).

[38] A. I. Kuznetsov, A. E. Miroshnichenko, M. L. Brongersma, Y. S. Kivshar, and B. Lukyanchuk, Optically resonant dielectric nanostructures, Science **354**, aag2472 (2016).

[39] K. Koshelev, S. Kruk, E. Melik-Gaykazyan, J.-H. Choi, A. Bogdanov, H.-G. Park, and Y. Kivshar, Subwavelength dielectric resonators for nonlinear nanophotonics, Science **367**, 288 (2020).

[40] M. V. Rybin, K. L. Koshelev, Z. F. Sadrieva, K. B. Samusev, A. A. Bogdanov, M. F. Limonov, and Y. S. Kivshar, High-q Supercavity Modes in Subwavelength Dielectric Resonators, Phys. Rev. Lett. **119**, 243901 (2017).

[41] R. Verre, D. G. Baranov, B. Munkhbat, J. Cuadra, M. Kall, and T. Shegai, Transition metal dichalcogenide nanodisks as high-index dielectric mie nanoresonators, Nat. Nanotechnol. **14**, 679 (2019).

[42] D. G. Baranov, D. A. Zuev, S. I. Lepeshov, O. V. Kotov, A. E. Krasnok, A. B. Evlyukhin, and B. N. Chichkov, All-dielectric nanophotonics: The quest for better materials and fabrication techiques, Optica **4**, 814 (2017).

[43] A. Arbabi, Y. Horie, M. Bagheri, and A. Faraon, Dielectric metasurfaces for complete control of phase and polarization with subwavelength spatial resolution and high transmission, Nat. Nanotechnol. **10**, 937 (2015).

[44] D. Lin, P. Fan, E. Hasman, and M. L. Brongersma, Dielectric gradient metasurface optical elements, Science **345**, 298 (2014).

[45] S. Kruk and Y. Kivshar, Functional meta-optics and nanophotonics governed by mie resonances, ACS Photonics **4**, 2638 (2017).

[46] S. S. Kruk, R. Camacho-Morales, L. Xu, M. Rahmani, D. A. Smirnova, L. Wang, H. H. Tan, C. Jagadish, D. N. Neshev, and Y. S. Kivshar, Nonlinear optical magnetism revealed by second-harmonic generation in nanoantennas, Nano Lett. **17**, 3914 (2017).

[47] V. F. Gili, L. Carletti, A. Locatelli, D. Rocco, M. Finazzi, L. Ghirardini, I. Favero, C. Gomez, A. Lemaitre, M. Celebrano, C. De Angelis, and G. Leo, Monolithic algaas second-harmonic nanoantennas, Opt. Express **24**, 15965 (2016).

[48] J. Cambiasso, G. Grinblat, Y. Li, A. Rakovich, E. Cortes, and S. A. Maier, Bridging the gap between dielectric nanophotonics and the visible regime with effectively lossless gallium phosphide antennas, Nano Lett. **17**, 1219 (2017).

[49] W. L. Barnes, A. Dereux, and T. W. Ebbesen, Surface plasmon subwavelength optics, Nature (London) **424**, 824 (2003).

[50] T. W. Ebbesen, H. J. Lezec, H. F. Ghaemi, T. Thio, and P. A. Wolff, Extraordinary optical transmission through sub-wavelength hole arrays, Nature (London) **391**, 667 (1998).

[51] D. K. Gramotnev and S. I. Bozhevolnyi, Plasmonics beyond the diffraction limit, Nat. Photonics **4**, 83 (2010).

[52] J. A. Schuller, E. S. Barnard, W. Cai, Y. C. Jun, J. S. White, and M. L. Brongersma, Plasmonics for extreme light concentration and manipulation, Nat. Mater. **9**, 193 (2010).

[53] S. A. Maier, *Plasmonics: Fundamentals and Applications* (Springer, New York, 2007), Vol. 1, p. 245.

[54] M. S. Tame, K. R. McEnery, S. K. Ozdemir, J. Lee, S. A. Maier, and M. S. Kim, Quantum plasmonics, Nat. Phys. **9**, 329 (2013).

[55] J. B. Khurgin, How to deal with the loss in plasmonics and metamaterials, Nat. Nanotechnol. **10**, 2 (2015).

[56] J. B. Khurgin and A. Boltasseva, Reflecting upon the losses in plasmonics and metamaterials, MRS Bull. **37**, 768 (2012).

[57] O. Hess, J. B. Pendry, S. A. Maier, R. F. Oulton, J. M. Hamm, and K. L. Tsakmakidis, Active nanoplasmonics metamaterials, Nat. Mater. **11**, 573 (2012).

[58] J. B. Khurgin and G. Sun, Practicality of compensating the loss in the plasmonic waveguides using semiconductor gain medium, Appl. Phys. Lett. **100**, 011105 (2012).

[59] L. Ge, Y. D. Chong, S. Rotter, H. E. Tureci, and A. D. Stone, Unconventional modes in lasers with spatially varying gain and loss, Phys. Rev. A **84**, 023820 (2011).

[60] M. Liertzer, L. Ge, A. Cerjan, A. D. Stone, H. E. Tureci, and S. Rotter, Pump-Induced Exceptional Points in Lasers, Phys. Rev. Lett. **108**, 173901 (2012).
[61] R. El-Ganainy, K. G. Makris, D. N. Christodoulides, and Z. H. Musslimani, Theory of coupled optical PT-symmetric structures, Opt. Lett. **32**, 2632 (2007).
[62] S. Klaiman, U. Gunther, and N. Moiseyev, Visualization of Branch Points in PT-Symmetric Waveguides, Phys. Rev. Lett. **101**, 080402 (2008).
[63] K. G. Makris, R. El-Ganainy, D. N. Christodoulides, and Z. H. Musslimani, Beam Dynamics in PT Symmetric Optical Lattices, Phys. Rev. Lett. **100**, 103904 (2008).
[64] A. Guo, G. J. Salamo, D. Duchesne, R. Morandotti, M. Volatier-Ravat, V. Aimez, G. A. Siviloglou, and D. N. Christodoulides, Observation of PT-Symmetry Breaking in Complex Optical Potentials, Phys. Rev. Lett. **103**, 093902 (2009).
[65] C. E. Ruter, K. G. Makris, R. El-Ganainy, D. N. Christodoulides, M. Segev, and D. Kip, Observation of parity-time symmetry in optics, Nat. Phys. **6**, 192 (2010).
[66] A. Regensburger, C. Bersch, M. A. Miri, G. Onishchukov, D. N. Christodoulides, and U. Peschel, Parity-time synthetic photonic lattices, Nature (London) **488**, 167 (2012).
[67] B. Peng, S. K. Ozdemir, F. Lei, F. Monifi, M. Gianfreda, G. L. Long, S. Fan, F. Nori, C. M. Bender, and L. Yang, Parity-time-symmetric whispering-gallery microcavities, Nat. Phys. **10**, 394 (2014).
[68] Z. H. Musslimani, K. G. Makris, R. El-Ganainy, and D. N. Christodoulides, Optical Solitons in PT Periodic Potentials, Phys. Rev. Lett. **100**, 030402 (2008).
[69] V. V. Konotop, J. Yang, and D. A. Zezyulin, Nonlinear waves in PT-symmetric systems, Rev. Mod. Phys. **88**, 035002 (2016).
[70] S. Longhi, Bloch Oscillations in Complex Crystals with PT Symmetry, Phys. Rev. Lett. **103**, 123601 (2009).
[71] L. Feng, R. El-Ganainy, and L. Ge, Non-hermitian photonics based on parity-time symmetry, Nat. Photonics **11**, 752 (2017).
[72] R. El-Ganainy, K. G. Makris, M. Khajavikhan, Z. H. Musslimani, S. Rotter, and D. N. Christodoulides, Non-hermitian physics and PT symmetry., Nat. Phys. **14**, 11 (2018).
[73] A. A. Zyablovsky, A. P. Vinogradov, A. A. Pukhov, A. V. Dorofeenko, and A. A. Lisyansky, PT-symmetry in optics, Phys. Usp. **57**, 1063 (2014).
[74] A. A. Zyablovsky, E. S. Andrianov, and A. A. Pukhov, Parametric instability of optical non-Hermitian systems near the exceptional point, Sci. Rep. **6**, 29709 (2016).
[75] M. A. Miri and A. Alu, Exceptional points in optics and photonics, Science **363**, eaar7709 (2019).
[76] S. Longhi, Pt-symmetric laser absorber, Phys. Rev. A **82**, 031801(R) (2010).
[77] B. Peng, S. K. Ozdemir, S. Rotter, H. Yilmaz, M. Liertzer, F. Monifi, C. M. Bender, F. Nori, and L. Yang, Loss-induced suppression and revival of lasing, Science **346**, 328 (2014).
[78] L. Feng, Z. J. Wong, R. M. Ma, Y. Wang, and X. Zhang, Single-mode laser by parity-time symmetry breaking, Science **346**, 972 (2014).
[79] H. Hodaei, M. A. Miri, M. Heinrich, D. N. Christodoulides, and M. Khajavikhan, Parity-time-symmetric microring lasers, Science **346**, 975 (2014).
[80] A. A. Zyablovsky, I. V. Doronin, E. S. Andrianov, A. A. Pukhov, Y. E. Lozovik, A. P. Vinogradov, and A. A. Lisyansky, Exceptional points as lasing prethresholds, Laser Photonics Rev. **15**, 2000450 (2021).
[81] H. Hodaei, A. U. Hassan, S. Wittek, H. Garcia-Gracia, R. El-Ganainy, D. N. Christodoulides, and M. Khajavikhan, Enhanced sensitivity at higher-order exceptional points, Nature (London) **548**, 187 (2017).
[82] J. Wiersig, Enhancing the Sensitivity of Frequency and Energy Splitting Detection by Using Exceptional Points: Application to Microcavity Sensors for Single-Particle Detection, Phys. Rev. Lett. **112**, 203901 (2014).
[83] W. Chen, S. K. Ozdemir, G. Zhao, J. Wiersig, and L. Yang, Exceptional points enhance sensing in an optical microcavity, Nature (London) **548**, 192 (2017).
[84] M. Zhang, W. Sweeney, C. W. Hsu, L. Yang, A. D. Stone, and L. Jiang, Quantum Noise Theory of Exceptional Point Amplifying Sensors, Phys. Rev. Lett. **123**, 180501 (2019).
[85] Z. Lin, H. Ramezani, T. Eichelkraut, T. Kottos, H. Cao, and D. N. Christodoulides, Unidirectional Invisibility Induced by PT-Symmetric Periodic Structures, Phys. Rev. Lett. **106**, 213901 (2011).
[86] L. Feng, Y. L. Xu, W. S. Fegadolli, M. H. Lu, J. E. Oliveira, V. R. Almeida, Y.-F. Chen, and A. Scherer, Experimental demonstration of a unidirectional reflectionless parity-time metamaterial at optical frequencies, Nat. Mater. **12**, 108 (2013).
[87] H. Ramezani, T. Kottos, R. El-Ganainy, and D. N. Christodoulides, Unidirectional nonlinear PT-symmetric optical structures, Phys. Rev. A **82**, 043803 (2010).
[88] L. Feng, M. Ayache, J. Huang, Y. L. Xu, M. H. Lu, Y. F. Chen, Y. Fainman, and A. Scherer, Nonreciprocal light propagation in a silicon photonic circuit, Science **333**, 729 (2011).
[89] Y. D. Chong, L. Ge, and A. D. Stone, PT-Symmetry Breaking and Laser-Absorber Modes in Optical Scattering Systems, Phys. Rev. Lett. **106**, 093902 (2011).
[90] D. Jalas, A. Petrov, M. Eich, W. Freude, S. Fan, Z. Yu, R. Baets, M. Popovic, A. Melloni, J. D. Joannopoulos, M. Vanwolleghem, C. R. Doerr, and H. Renner, What is-and what is not-an optical isolator, Nat. Photonics **7**, 579 (2013).
[91] A. V. Dorofeenko, A. A. Zyablovsky, A. A. Pukhov, A. A. Lisyansky, and A. P. Vinogradov, Light propagation in composite materials with gain layers, Phys. Usp. **55**, 1080 (2012).
[92] Y. D. Chong, L. Ge, H. Cao, and A. D. Stone, Coherent Perfect Absorbers: Time-Reversed Lasers, Phys. Rev. Lett. **105**, 053901 (2010).
[93] M. T. Hill and M. C. Gather, Advances in small lasers, Nat. Photonics **8**, 908 (2014).
[94] A. J. Kuehne and M. C. Gather, Organic lasers: Recent developments on materials, device geometries, and fabrication techniques, Chem. Rev. **116**, 12823 (2016).
[95] R. Matloob, R. Loudon, M. Artoni, S. M. Barnett, and J. Jeffers, Electromagnetic field quantization in amplifying dielectrics, Phys. Rev. A **55**, 1623 (1997).

[96] See Supplemental Material at http://link.aps.org/supplemental/10.1103/PhysRevLett.129.133901 for details of numerical simulation of lasing in a subwavelength dielectric layer.

[97] A. A. Zyablovsky, A. P. Vinogradov, A. V. Dorofeenko, A. A. Pukhov, and A. A. Lisyansky, Causality and phase transitions in PT-symmetric optical systems, Phys. Rev. A **89**, 033808 (2014).

[98] S. S. Mirshafieyan, T. S. Luk, and J. Guo, Zeroth order fabry-perot resonance enabled ultra-thin perfect light absorber using percolation aluminum and silicon nanofilms, Opt. Mater. Express **6**, 1032 (2016).

[99] A. A. Zyablovsky, I. A. Nechepurenko, E. S. Andrianov, A. V. Dorofeenko, A. A. Pukhov, A. P. Vinogradov, and A. A. Lisyansky, Optimum gain for plasmonic distributed feedback lasers, Phys. Rev. B **95**, 205417 (2017).

[100] N. Kirstaedter, O. Schmidt, N. Ledentsov, D. Bimberg, V. Ustinov, A. Y. Egorov, A. Zhukov, M. Maximov, P. Kop'ev, and Z. I. Alferov, Gain and differential gain of single layer inas/gaas quantum dot injection lasers, Appl. Phys. Lett. **69**, 1226 (1996).

[101] O. Schmidt, N. Kirstaedter, N. Ledentsov, M.-H. Mao, D. Bimberg, V. Ustinov, A. Y. Egorov, A. Zhukov, M. Maximov, P. Kop'ev *et al.*, Prevention of gain saturation by multi-layer quantum dot lasers, Electron. Lett. **32**, 1302 (1996).

[102] L. Pavesi, L. Dal Negro, C. Mazzoleni, G. Franzo, and d. F. Priolo, Optical gain in silicon nanocrystals, Nature (London) **408**, 440 (2000).

[103] K.-Y. Jeong, M.-S. Hwang, J. Kim, J.-S. Park, J. M. Lee, and H.-G. Park, Recent progress in nanolaser technology, Adv. Mater. **32**, 2001996 (2020).

[104] K. Hirose, Y. Liang, Y. Kurosaka, A. Watanabe, T. Sugiyama, and S. Noda, Watt-class high-power, high-beam-quality photonic-crystal lasers, Nat. Photonics **8**, 406 (2014).

[105] A. Kodigala, T. Lepetit, Q. Gu, B. Bahari, Y. Fainman, and B. Kanté, Lasing action from photonic bound states in continuum, Nature (London) **541**, 196 (2017).

[106] S. T. Ha, Y. H. Fu, N. K. Emani, Z. Pan, R. M. Bakker, R. Paniagua-Domínguez, and A. I. Kuznetsov, Directional lasing in resonant semiconductor nanoantenna arrays, Nat. Nanotechnol. **13**, 1042 (2018).

[107] Y. Ota, K. Takata, T. Ozawa, A. Amo, Z. Jia, B. Kante, M. Notomi, Y. Arakawa, and S. Iwamoto, Active topological photonics, Nanophotonics **9**, 547 (2020).